Supplementary Material and methods

Flow cytometric analysis

Cells were dissociated with trypsin and resuspended at 1×10^6 cells/ml in DMEM containing 2% FBS and then pre-incubated at 37°C for 30 minutes with or without 100 μM verapamil (Sigma) to inhibit ABC transporters. The cells were subsequently incubated for 90 minutes at 37°C with Hoechst 33342 (5 μg/ml, Sigma). Finally, the cells were incubated on ice for 10 minutes and washed with ice-cold PBS before flow cytometric analysis. Flow cytometry data were analyzed by FlowJo 7.6.1 software.

Supplementary Figure Legends

Figure S1. RPRPD1A is downregulated in metastatic breast cancer and suppresses Wnt/β-catenin signaling activity. (A) Western blotting analysis of RPRD1A in the indicated cells. α-tubulin served as the loading control. **(B)** Growth curves of the MDA-MB-231/vector and MDA-MB-231/RPRD1A. **(C)** The expression of Wnt/β-catenin signaling downstream target genes analyzed by real-time quantitative PCR. Each bar represents the mean ± SD value from three independent experiments.

Figure S2. RPRD1A mRNA levels were not significantly altered in breast cancer. (A) Analyses of RPRD1A mRNA levels in published microarray data (TCGA, NCBI/GEO/GSE10797, 9574, 5764; $P > 0.05$). **(B)** RPRD1A mRNA levels in eight clinical breast cancer samples (T) paired with their corresponding adjacent non-tumor (ANT) tissues. (**C**) Expression of miR-454-3p in indicated cells. Each bar represents the mean ± SD value from three independent experiments.

Figure S3. miR-454-3p activates Wnt/β-catenin signaling. (A) A gene set enrichment analysis plot showing that miR-454-3p expression was correlated with related gene signatures in the Wnt/β-catenin pathway. **(B)** The expression of Wnt/β-catenin signaling downstream target genes in the indicated cells, analyzed by real-time quantitative PCR. **(C)** Western blotting analysis of RPRD1A in the indicated cells. α-tubulin served as the loading control.

Figure S4. MiR-454-3p promotes breast cancer metastasis. (A) Expression of miR-454-3p in human breast cancer clinical specimens from the TCGA miRNA expression array data. **(B)** Kaplan-Meier curves for breast cancer patients with low and high expression of miR-454-3p from the TCGA miRNA expression array data. **(C)** A gene set enrichment analysis plot showing that miR-454-3p expression was correlated with related gene signatures in tumor metastasis. **(D)** The expression of miR-454-3p and β-catenin, determined by real-time PCR

and western blotting respectively. β-catenin-RNAi#2 was chosen for further investigation. **(E and F)** Expression of miR-454-3p in exosomes (E) and circulating tumor cells (CTCs) (F) in peripheral blood circulation, determined by real-time quantitative PCR. Each bar represents the mean ± SD value from three independent experiments.

Figure S5. miR-454-3p contributes to early events in the breast cancer metastasis cascade. (A) Cell invasion assays of the indicated cells. **(B)** Cell morphology of MCF7 and ZR-75-1 cells overexpressing miR-454-3p. Each bar represents the mean ± SD value from three independent experiments. * $P < 0.05$.

Figure S6. miR-454-3p promotes early distant relapse in breast cancer. (A) A gene set enrichment analysis plot showing that miR-454 expression was correlated with related gene signatures in stem cells. **(B)** Expression of the stemness-associated genes *MYC*, *SOX2*, *OCT4*, *NANOG* and *SNAIL* in the indicated cells, analyzed by real-time quantitative PCR. **(C)** Hoechst33342 dye exclusion assay showing the proportion of SP^+ cells for the indicated cell groups. **(D)** Effect of miR-454-3p on *in vivo* tumorigenicity of the indicated breast cancer cells. Each bar represents the mean ± SD value from three independent experiments. * $P < 0.05$.

Figure S7. miR-454-3p is amplified in multiple types of tumors and promotes Wnt/β-catenin signaling activity. (A) The amplification rate of miR-454 in a subset of human tumors from the TCGA dataset. **(B)** Expression of miR-454 in a subset of human tumors from the TCGA dataset, in comparison with normal tissues. **(C)** Expression of miR-454 at different amplification levels in LIHC and KIRC samples from the TCGA dataset. **(D and E)** Kaplan-Meier curves for LIHC and KIRC patients from the TCGA dataset with low and high miR-454 expression. **(F)** Luciferase assay of TCF/LEF transcriptional activity in HepG2 and Caki-1 cells (left); quantification of tumor spheres formed from HepG2 and

Caki-1 cells (right). Each bar represents the mean ± SD value from three independent experiments. *$P < 0.05$.

Supplementary Tables

Table S1. Clinicopathological characteristics of studied breast cancer patients

Factor	**No.**	**(%)**
Age (years)		
≤ 53	162	69.8
> 53	70	30.1
Clinical stage		
I	39	16.8
II	107	46.1
III	76	32.8
IV	10	4.3
T classification		
T_1	67	28.9
T_2	119	51.3
T_3	32	13.8
T_4	14	6.0
N classification		
N_0	94	40.5
N_1	70	30.2
N_2	42	18.1
N3	26	11.2
M classification		
No	223	96.1
Yes	9	3.9
Vital status		
Alive	157	67.7
Dead	75	32.3
Expression of RPRD1A		
Low expression	122	52.6
High expression	110	47.4
Expression of miR-454-3p		
Low expression	116	50.0

High expression	116	50.0

Table S2. Correlation between the clinicopathological features and expression of RPRD1A

Patient characteristics		RPRD1A expression		*P*-value
		Low	High	
Age (years)	≤ 53	80	82	0.137
	> 53	42	28	
Clinical stage	I	4	35	< 0.001
	II	37	70	
	III	72	4	
	IV	9	1	
T classification	T_1	14	53	< 0.001
	T_2	67	52	
	T_3	29	3	
	T_4	12	2	
N classification	N_0	21	73	< 0.001
	N_1	39	31	
	N_2	37	5	
	N3	25	1	
M classification	No	114	109	0.026
	Yes	8	1	
Vital status	Alive	63	94	< 0.001
	Dead	59	16	

Table S3. Univariate and multivariate analysis of different prognostic parameters in patients with breast cancer by Cox-regression analysis

	Univariate analysis			Multivariate analysis		
	No. patients	*P*	Regression coefficient (SE)	*P*	Relative risk	95% confidence interval
Age						
≤ 53	162	0.002	0.009	0.074	1.019	1.001-1.036
> 53	70					
Clinical stage						
I	39					
II	107	< 0.001	0.053	0.435	1.405	0.908-1.202
III	76					
IV	10					
Expression of PRPD1A						
Low expression	122	< 0.001	0.288	0.002	0.409	0.206-0.812
High expression	110					
Expression of miR-454-3p						
Low expression	116	< 0.001	0.354	< 0.001	5.682	2.630-12.274
High expression	116					

Figure S1

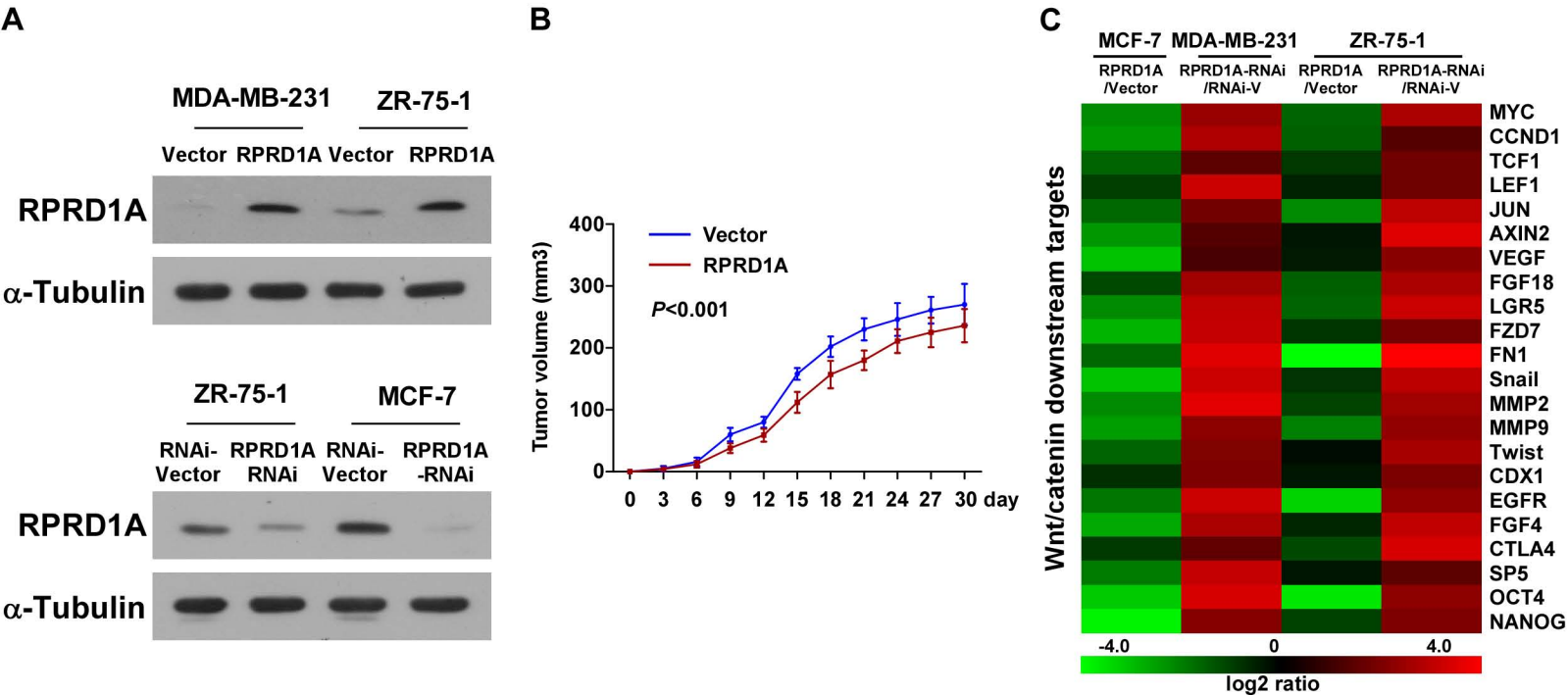
A
MDA-MB-231
ZR-75-1
Vector
RPRD1A
Vector
RPRD1A
RPRD1A
α-Tubulin
ZR-75-1
MCF-7
RNAi-Vector
RPRD1A RNAi
RNAi-Vector
RPRD1A -RNAi
RPRD1A
α-Tubulin
B
Tumor volume (mm3)
400
300
200
100
0
Vector
RPRD1A
P<0.001
0 3 6 9 12 15 18 21 24 27 30 day
C
MCF-7
MDA-MB-231
ZR-75-1
RPRD1A /Vector
RPRD1A-RNAi /RNAi-V
RPRD1A /Vector
RPRD1A-RNAi /RNAi-V
Wnt/catenin downstream targets
MYC
CCND1
TCF1
LEF1
JUN
AXIN2
VEGF
FGF18
LGR5
FZD7
FN1
Snail
MMP2
MMP9
Twist
CDX1
EGFR
FGF4
CTLA4
SP5
OCT4
NANOG
-4.0
0
4.0
log2 ratio

Figure S2

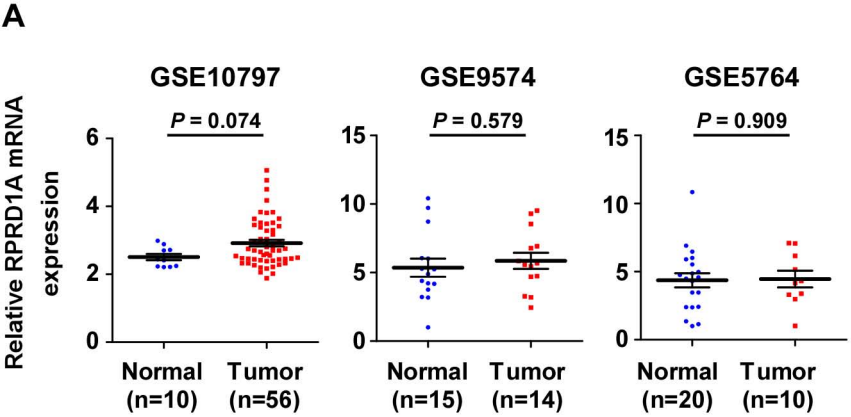
A
GSE10797
GSE9574
GSE5764
P = 0.074
P = 0.579
P = 0.909
Relative RPRD1A mRNA expression
Normal (n=10)
Tumor (n=56)
Normal (n=15)
Tumor (n=14)
Normal (n=20)
Tumor (n=10)

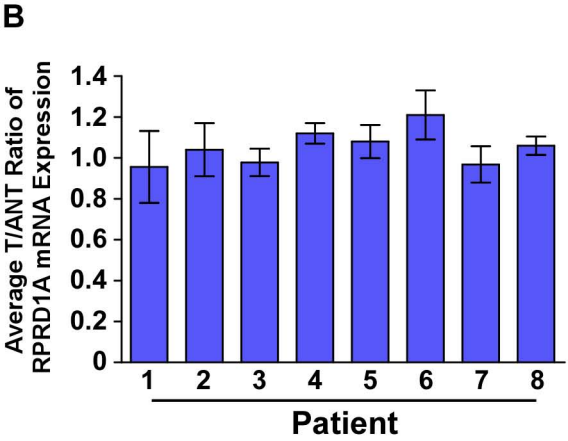
B
Average T/ANT Ratio of RPRD1A mRNA Expression
Patient

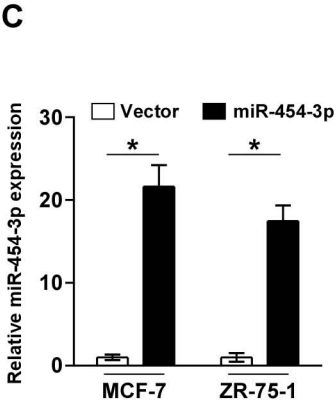
C
Vector
miR-454-3p
Relative miR-454-3p expression
MCF-7
ZR-75-1

Figure S3

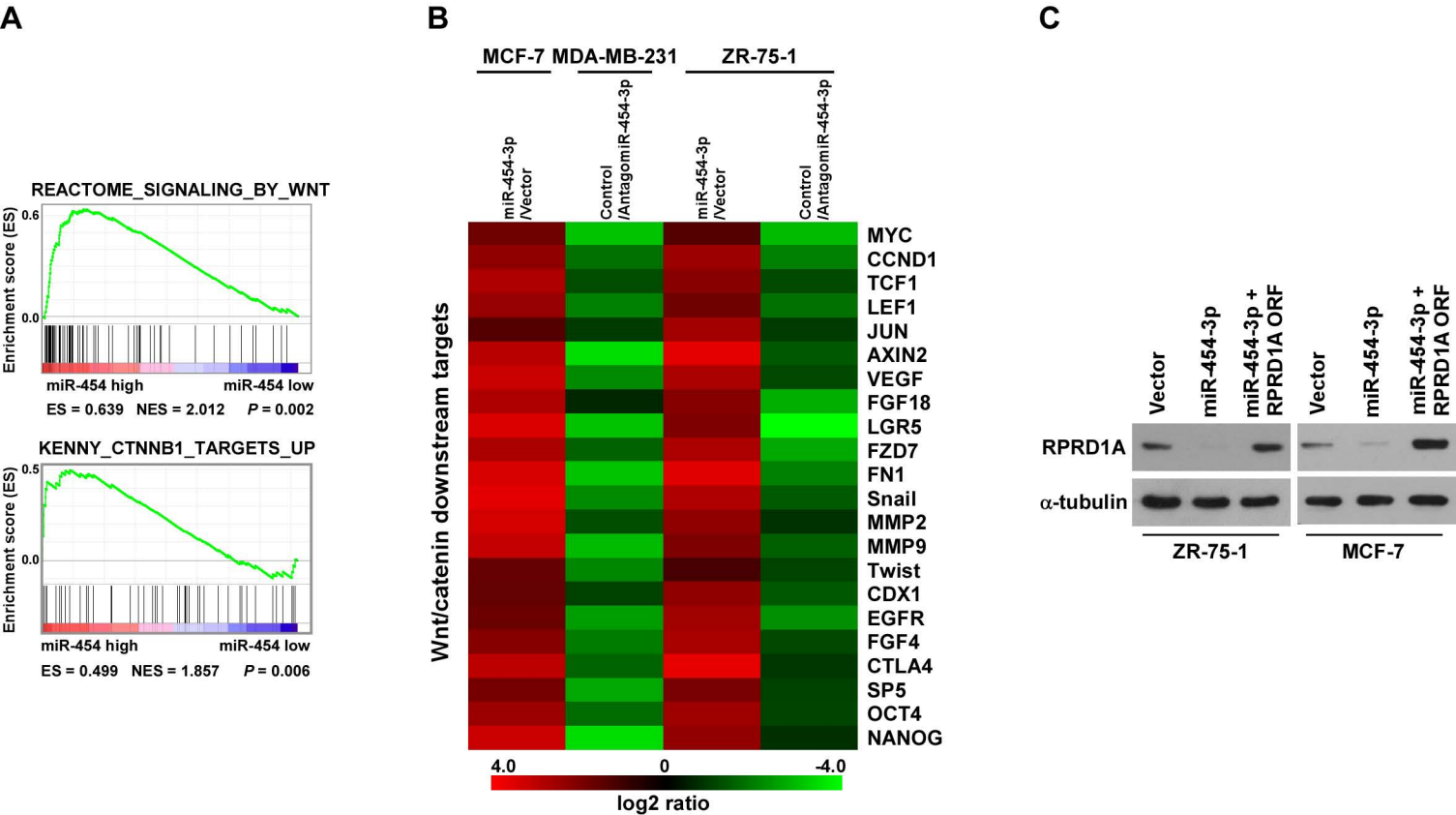
A
REACTOME_SIGNALING_BY_WNT
Enrichment score (ES)
0.6
0.0
miR-454 high
miR-454 low
ES = 0.639 NES = 2.012 P = 0.002
KENNY_CTNNB1_TARGETS_UP
Enrichment score (ES)
0.5
0.0
miR-454 high
miR-454 low
ES = 0.499 NES = 1.857 P = 0.006
B
MCF-7
MDA-MB-231
ZR-75-1
miR-454-3p /Vector
Control /AntagomiR-454-3p
miR-454-3p /Vector
Control /AntagomiR-454-3p
Wnt/catenin downstream targets
MYC
CCND1
TCF1
LEF1
JUN
AXIN2
VEGF
FGF18
LGR5
FZD7
FN1
Snail
MMP2
MMP9
Twist
CDX1
EGFR
FGF4
CTLA4
SP5
OCT4
NANOG
4.0
0
-4.0
log2 ratio
C
Vector
miR-454-3p
miR-454-3p + RPRD1A ORF
Vector
miR-454-3p
miR-454-3p + RPRD1A ORF
RPRD1A
α-tubulin
ZR-75-1
MCF-7

Figure S4

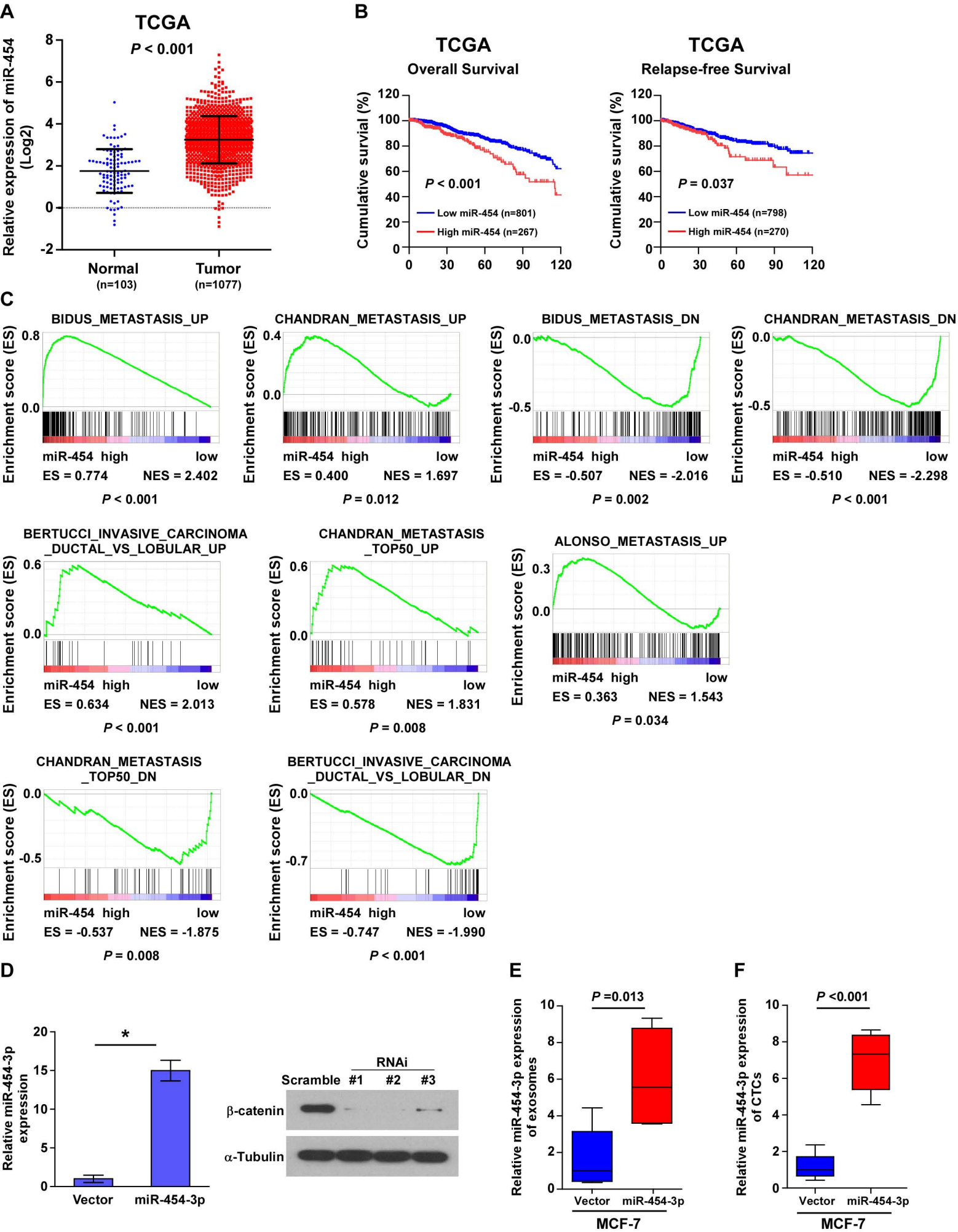
A
TCGA
P < 0.001
Relative expression of miR-454 (Log2)
Normal (n=103)
Tumor (n=1077)
B
TCGA
Overall Survival
Cumulative survial (%)
P < 0.001
Low miR-454 (n=801)
High miR-454 (n=267)
TCGA
Relapse-free Survival
P = 0.037
Low miR-454 (n=798)
High miR-454 (n=270)
C
BIDUS_METASTASIS_UP
Enrichment score (ES)
miR-454 high low
ES = 0.774 NES = 2.402
P < 0.001
CHANDRAN_METASTASIS_UP
ES = 0.400 NES = 1.697
P = 0.012
BIDUS_METASTASIS_DN
ES = -0.507 NES = -2.016
P = 0.002
CHANDRAN_METASTASIS_DN
ES = -0.510 NES = -2.298
P < 0.001
BERTUCCI_INVASIVE_CARCINOMA_DUCTAL_VS_LOBULAR_UP
ES = 0.634 NES = 2.013
P < 0.001
CHANDRAN_METASTASIS_TOP50_UP
ES = 0.578 NES = 1.831
P = 0.008
ALONSO_METASTASIS_UP
ES = 0.363 NES = 1.543
P = 0.034
CHANDRAN_METASTASIS_TOP50_DN
ES = -0.537 NES = -1.875
P = 0.008
BERTUCCI_INVASIVE_CARCINOMA_DUCTAL_VS_LOBULAR_DN
ES = -0.747 NES = -1.990
P < 0.001
D
Relative miR-454-3p expression
*
Vector miR-454-3p
RNAi
Scramble #1 #2 #3
β-catenin
α-Tubulin
E
Relative miR-454-3p expression of exosomes
P =0.013
Vector miR-454-3p
MCF-7
F
Relative miR-454-3p expression of CTCs
P <0.001
Vector miR-454-3p
MCF-7

Figure S5

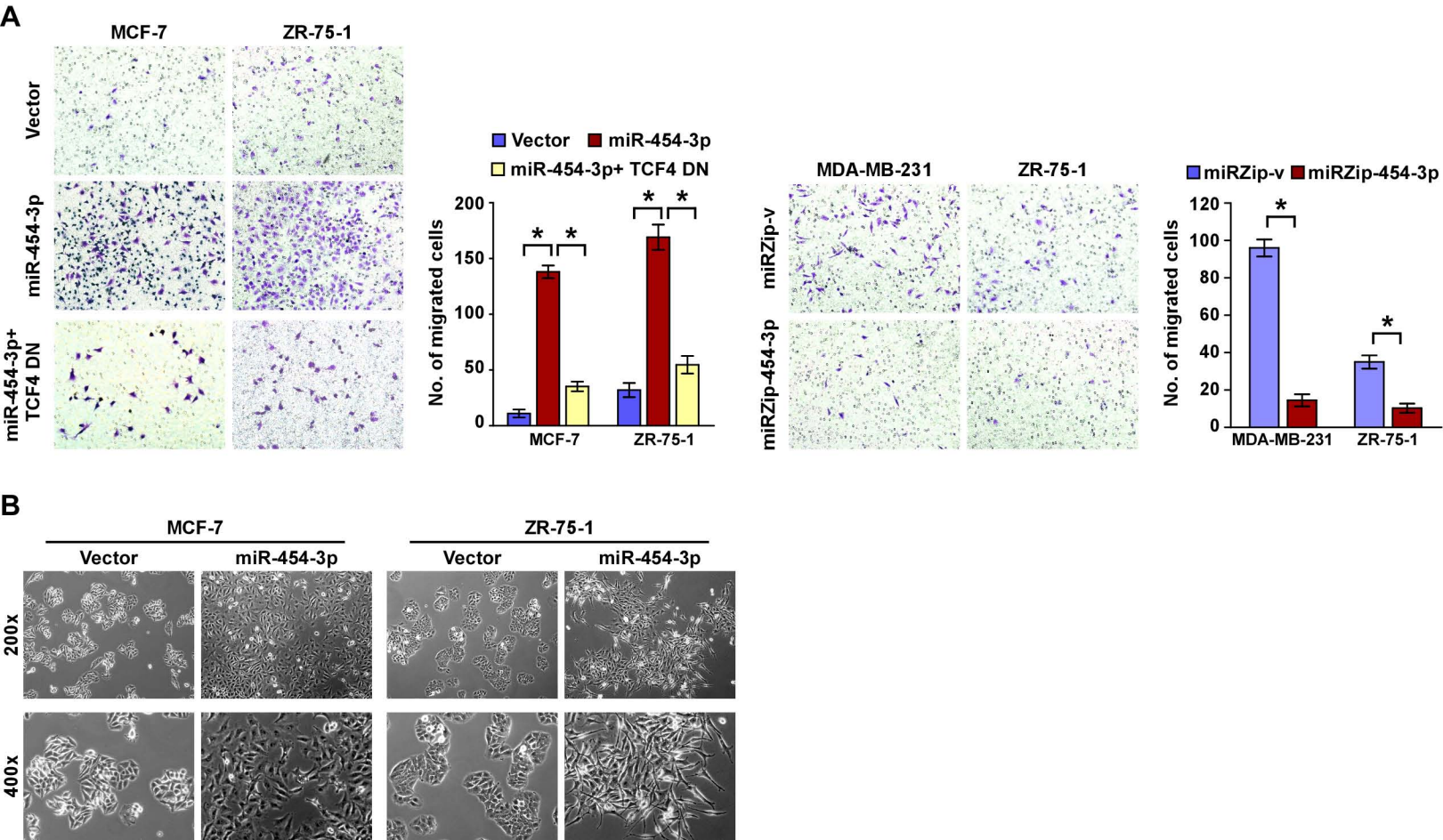
A
MCF-7
ZR-75-1
Vector
miR-454-3p
miR-454-3p+ TCF4 DN
Vector
miR-454-3p
miR-454-3p+ TCF4 DN
No. of migrated cells
200
150
100
50
0
MCF-7
ZR-75-1
MDA-MB-231
ZR-75-1
miRZip-v
miRZip-454-3p
miRZip-v
miRZip-454-3p
No. of migrated cells
120
100
80
60
40
20
0
MDA-MB-231
ZR-75-1
B
MCF-7
ZR-75-1
Vector
miR-454-3p
Vector
miR-454-3p
200x
400x

Figure S6

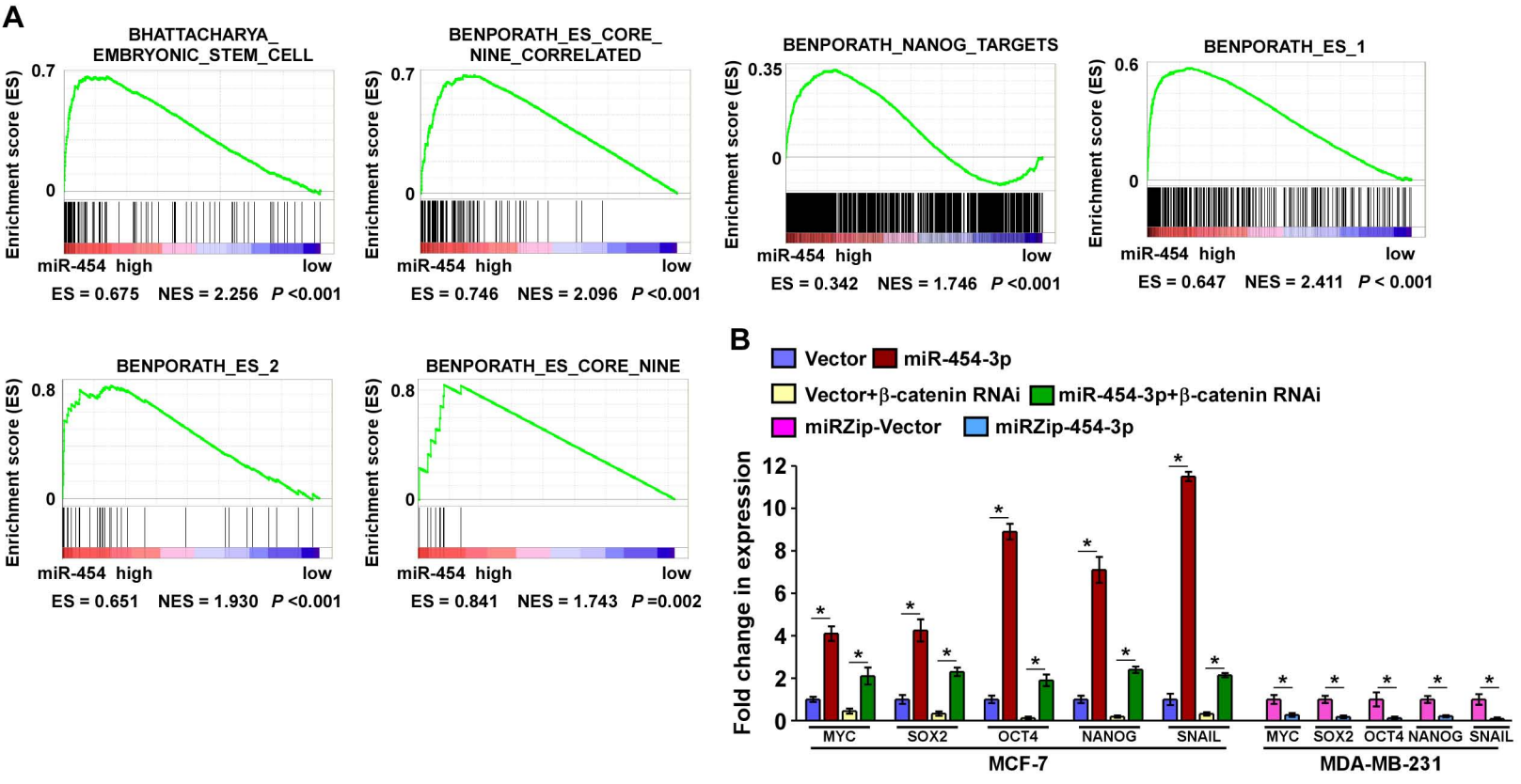

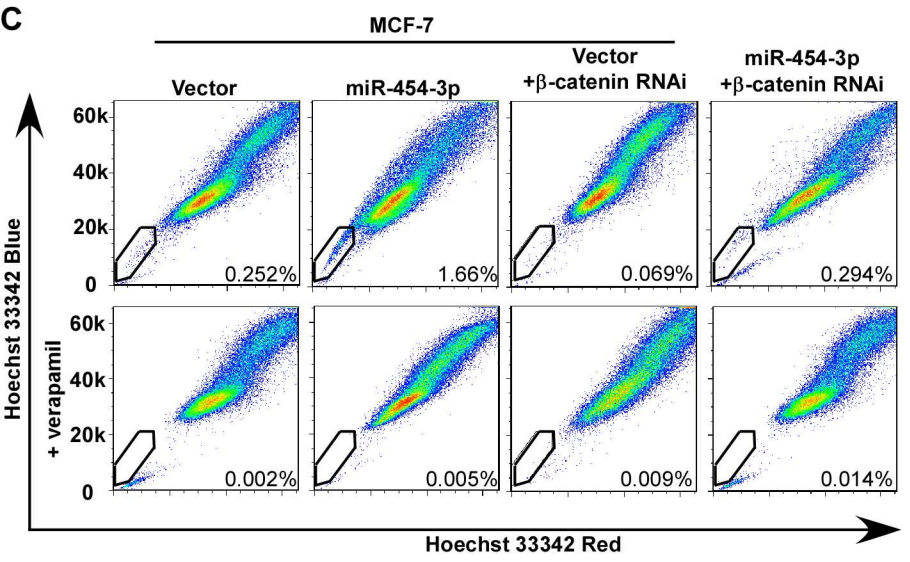

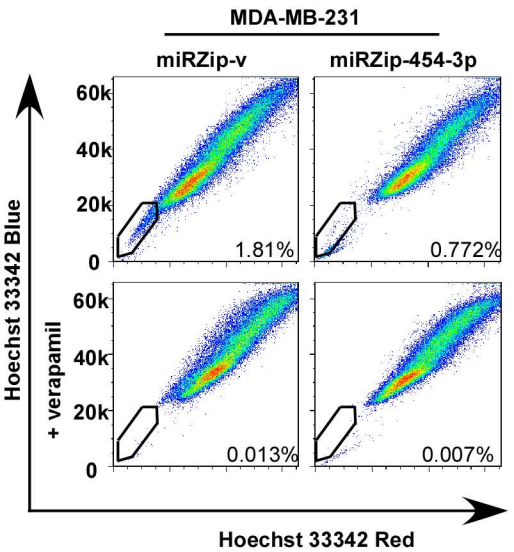

D

Cell type	Cell number	Tumor incidence	TIC Frequency (95% CI)	*P* value
MCF-7				
Vector	1000000	4/8	1/1089366 (1/2550058-1/465370)	< 0.001
	100000	2/8		
	10000	0/12		
	1000	0/12		
	500	0/15		
miR-454-3p	1000000	7/8	1/201174 (1/477982-1/84671)	
	100000	5/8		
	10000	2/12		
	1000	1/12		
	500	0/15		
Vector+ β-catenin RNAi	1000000	1/8	1/8468934 (1/60102376-1/1193345)	< 0.001
	100000	0/8		
	10000	0/12		
	1000	0/12		
	500	0/15		
miR-454-3p+ β-catenin RNAi	1000000	5/8	1/996213 (1/2286372-1/434068)	
	100000	1/8		
	10000	0/12		
	1000	0/12		
	500	0/15		
MDA-MB-231				
miRZip-V	1000000	6/8	1/546350 (1/1164568-1/256317)	< 0.001
	100000	3/8		
	10000	0/12		
	1000	0/12		
	500	0/15		
miRZip-454-3p	1000000	2/8	1/2608593 (1/8294637-1/820381)	
	100000	1/8		
	10000	0/12		
	1000	0/12		
	500	0/15		

Figure S7

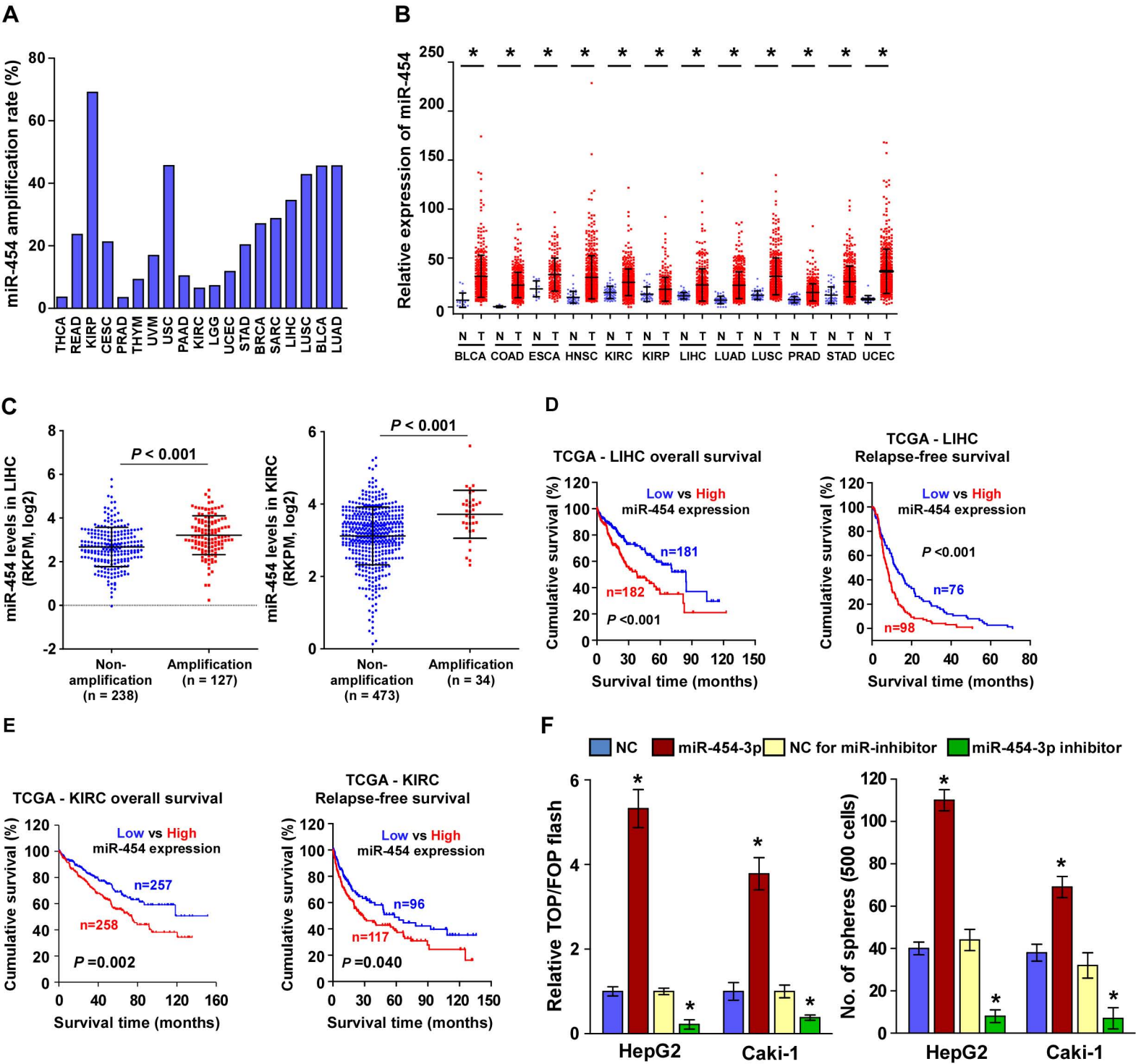
A
miR-454 amplification rate (%)
THCA
READ
KIRP
CESC
PRAD
THYM
UVM
USC
PAAD
KIRC
LGG
UCEC
STAD
BRCA
SARC
LIHC
LUSC
BLCA
LUAD
B
Relative expression of miR-454
N T
BLCA COAD ESCA HNSC KIRC KIRP LIHC LUAD LUSC PRAD STAD UCEC
C
miR-454 levels in LIHC (RKPM, log2)
P < 0.001
Non-amplification (n = 238)
Amplification (n = 127)
miR-454 levels in KIRC (RKPM, log2)
P < 0.001
Non-amplification (n = 473)
Amplification (n = 34)
D
TCGA - LIHC overall survival
Low vs High miR-454 expression
n=181
n=182
P <0.001
Cumulative survival (%)
Survival time (months)
TCGA - LIHC Relapse-free survival
Low vs High miR-454 expression
P <0.001
n=76
n=98
Cumulative survival (%)
Survival time (months)
E
TCGA - KIRC overall survival
Low vs High miR-454 expression
n=257
n=258
P =0.002
Cumulative survival (%)
Survival time (months)
TCGA - KIRC Relapse-free survival
Low vs High miR-454 expression
n=96
n=117
P =0.040
Cumulative survival (%)
Survival time (months)
F
NC
miR-454-3p
NC for miR-inhibitor
miR-454-3p inhibitor
Relative TOP/FOP flash
HepG2
Caki-1
No. of spheres (500 cells)
HepG2
Caki-1